npj | Materials Degradation

www.nature.com/npjmatdeg

ARTICLE OPEN

The contribution of hydrogen evolution processes during corrosion of aluminium and aluminium alloys investigated by potentiodynamic polarisation coupled with real-time hydrogen measurement

Christophe Laurent[1,2], Fabio Scenini[2], Tullio Monetta[3], Francesco Bellucci[3] and Michele Curioni[2]

Water reduction, which leads to the evolution of hydrogen, is a key cathodic process for corrosion of many metals of technological interest such as magnesium, aluminium, and zinc; and its understanding is critical for design of new alloys or protective treatments. In this work, real-time hydrogen evolution measurement was coupled with potentiodynamic measurements on high-purity aluminium and AA2024-T3 aluminium alloy. The results show that both materials exhibit superfluous hydrogen evolution during anodic polarisation and that the presence of cathodically active alloying elements enhances hydrogen evolution. Furthermore, it was observed for the first time that superfluous hydrogen evolution also occurs during cathodic polarisation. Both the anodic and cathodic behaviours can be rationalised by a model assuming that superfluous hydrogen evolution occurs locally where the naturally formed oxide is disrupted. Specifically, during anodic polarisation, oxide disruption is due to the combined presence of chloride ions and acidification, whereas during cathodic polarisation, such disruption is due to alkalinisation. Furthermore, the presence of cathodically active alloying elements enhances superfluous hydrogen evolution in response to either anodic or cathodic polarisation, and results in 'cathodic activation' of the dissolved regions.

npj Materials Degradation (2017)1:6 ; doi:10.1038/s41529-017-0011-4

INTRODUCTION

Aqueous corrosion is probably the most important single cause of materials degradation and it occurs by the simultaneous oxidation of metal and reduction of species present in the environment. In order to preserve charge neutrality, the oxidation (anodic) and reduction (cathodic) reactions must proceed at the same rate; consequently, the slower of the two processes determines the overall corrosion rate. For relatively noble materials, the most important cathodic reaction in practical cases is the reduction of oxygen dissolved in the aqueous environment. However, for more reactive materials, i.e. with a low electrochemical potential for metal oxidation such as zinc, aluminium and magnesium, the reduction of hydrogen cations from water is thermodynamically possible and might provide a substantial contribution to the overall corrosion rate.[1] In the case of magnesium immersed in an electrolyte, hydrogen evolution largely dominates on oxygen reduction, as the potential of magnesium in aqueous environments remains at all times «1 V vs. SHE. Thus, in many cases of practical interest, the corrosion rate of magnesium correlates well with the amount of hydrogen evolved.[2–9] For aluminium, hydrogen evolution can be triggered in specific environments typical of active corrosion sites such as, for example, pits or crevices,[10–20] increasing substantially the local corrosion rate. Besides corrosion, unwanted hydrogen evolution can be an important issue for other practical applications; for example, it is responsible for the reduction of the faradic efficiency of primary batteries and sacrificial anodes. Therefore, an improved understanding of the hydrogen evolution mechanism for both metals, and the identification of strategies to minimise it, would enable better alloy design and development of innovative protection measures.

This work quantitatively investigates the hydrogen evolution behaviour for high purity aluminium (99.99 %wt.) and a commercial aluminium–copper–magnesium alloy (AA2024-T3), with the aim of elucidating the fundamental mechanisms involved and the effects associated with the presence of a noble alloying element, such as copper.

Hydrogen evolution on aluminium and magnesium has received significant attention in recent years, due to its fundamental and technological relevance.[3, 4, 12, 16, 21–27] On these metals, with relatively low electrochemical potential for oxidation, hydrogen evolution is always thermodynamically possible in the presence of water, but may be hindered by the presence of an oxide, hydroxide, or mixed film that physically separates the metal surface from the electrolyte. In some conditions, when the film is locally disrupted, such as for example during anodic polarisation in chloride-containing environment or at active corrosion sites (pits) during free corrosion, hydrogen evolution might occur

[1]Department of Materials and Surface Treatment, ENSIL – University of Limoges, 33 rue François Mitterrand, Limoges 87032, France; [2]Corrosion and Protection Centre, School of Materials, University of Manchester, Oxford Road, Manchester M139PL, UK and [3]Dept. of Chemical Engineering, Materials and Industrial Production, University of Naples "Federico II", Naples 80125, Italy
Correspondence: Michele Curioni (michele.curioni@manchester.ac.uk)

Received: 7 February 2017 Revised: 4 April 2017 Accepted: 27 April 2017
Published online: 18 September 2017

Published in partnership with CSCP and USTB

npj nature partner journals

locally, providing additional current sustaining corrosion propagation.[12, 28]

The increase in hydrogen evolution rate during anodic polarisation, which is observed both for aluminium[14–19] and magnesium,[3, 4, 29, 30] is particularly evident and it has attracted significant interest, since it is contrary to what electrochemical theory would predict. The phenomenon is often referred to as 'negative difference effect' or 'superfluous' hydrogen evolution. In the case of aluminium, it appears that there is a correlation between the occurrence of superfluous hydrogen and the onset of pitting during polarisation or even during free corrosion.[14–19, 31] For example, Frankel observed abundant hydrogen evolution during the growth of 2-dimensional pits on aluminium [17] under anodic polarisation and estimated that the current associated with hydrogen evolution was approximately constant, regardless of the applied anodic potential. McCafferty[31] proposed a sequence of steps for the initiation and propagation of pitting on aluminium in the presence of chloride ions, and suggested that the formation of hydrogen gas might play a role in disrupting the passive film, by forming oxide blisters that rupture due to the high hydrogen pressure. Drazic et al. found that hydrogen evolution on aluminium decreased with increasing potential until the pitting potential, and abruptly increased above the pitting potential.[16, 18, 19] Frankel et al. also observed substantial increase in hydrogen evolution above the pitting potential, and obtained qualitatively similar conclusions to Drazic et al.[32] when polarising aluminium in concentrate HCl solutions.

Recent studies focusing on the hydrogen evolution behaviour of aluminium in acidified solution with and without depassivating chloride ions and/or in presence and absence of a galvanically coupled nobler material suggest that the superfluous hydrogen evolution requires the combined presence of: (i) a '*remote*' current (in the anodic direction at the corrosion front, that can be produced directly on the electrode surface by cathodic hydrogen evolution, or be provided by an external circuit), and (ii) of depassivating conditions, i.e. local acidification and/or presence of aggressive ion such as chlorides.[12, 22, 23, 28] A model was proposed, where the superfluous hydrogen evolution was generated at the active corrosion front, due to the local disruption of passivity, resulting either in the direct exposure of the metal to the electrolyte or in the formation of only a poorly protective chloride-rich film.[12, 28] At those locations, due to the large potential difference available locally, hydrogen evolution can take place and, overall, the corrosion front acts as a current amplifier, where the anodic current produced at some locations far from the corrosion front, i.e. remotely, induces a local cathodic reaction (hydrogen evolution). Consequently, the amount of metal oxidised is proportional to the sum of the '*remote*' anodic current and the additional current produced locally by hydrogen evolution. These findings suggest that hydrogen evolution within pits is not due exclusively to acidification, since the tests were performed in acidic solution, but it is associated with the breakdown of passivity, mainly triggered by the presence of chloride ions.

Aside from the phenomenon of the superfluous hydrogen evolution (that can only observed during anodic polarisation), it has also recently been shown that on alloys of practical interest such as AA2024-T3, the presence of a stable corrosion site is associated with the presence of hydrogen evolution at the corrosion front.[10, 11] This is due to the fact that, when favourable conditions are generated for stable evolution of hydrogen at or in proximity to the corrosion front, the rate at which corrosion propagates becomes no longer limited purely by the arrival of cathodic reactants on the macroscopic electrode surface, but is enhanced by the current amplification effect described earlier.[12] Similar considerations may also apply to crevice corrosion, where the local acidification and presence of chloride can promote the disruption of the oxide film, resulting in direct exposure of the underlying metal to the electrolyte, with consequent hydrogen evolution within the crevice and significant increase of the local corrosion rate.

In addition to the hydrogen evolution at the active corrosion front, an additional phenomenon, called 'cathodic activation', is sometime observed on aluminium, magnesium and various other metals, as recently systematically reported by Liu et al.[33] Cathodic activation is observed when the cathodic activity of corroded regions is significantly higher than the cathodic activity of uncorroded regions. The metal where this phenomenon is visually more evident is magnesium, where the surface changes from silvery, prior to corrosion, to dark, after corrosion, and on the dark surface the hydrogen evolution clearly proceed at a higher rate than on the silvery surface.[2–5, 21, 34] Thus, when cathodic activation takes place, the overall rate of hydrogen evolution at the free corrosion potential increases since there is an increase in hydrogen evolution occurring on the cathodically activated corroded regions, which result in increased availability of anodic current at the corrosion front which, in turn, results in further local hydrogen evolution.[12, 21, 23]

Based on the previous considerations, it is clear that understanding the details of hydrogen evolution can provide insight into the corrosion behaviour in simple and more complex alloys. For aluminium, however, the experimental investigation at the open circuit potential is not trivial since, during free corrosion, the amount of hydrogen evolved is relatively low, and difficult to measure directly. Consequently, for a fundamental study, it is more convenient to measure hydrogen evolution during electrochemical polarisation.

Experimentally, hydrogen evolution can be measured by using various methods, each with advantages and disadvantages,[2, 12, 21, 23] but for the purpose of correlating electrochemical response with hydrogen evolution, the gravimetric method [21–23, 25] is preferred, since it provides sufficient time and volume resolution and requires only readily available and inexpensive equipment. The method is based on the measurement of the weight of a completely submerged container that collects the hydrogen developed from the electrode (Fig. 1). By using the gravimetric

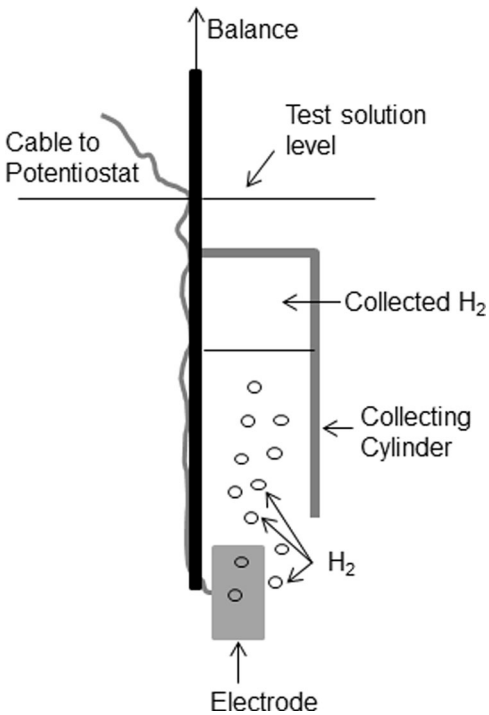

Fig. 1 Schematic representation of the experimental setup for real-time hydrogen measurement

method it is possible to directly compare the electrical current (anodic or cathodic) applied to the electrode, with the electrical current associated with the measured hydrogen evolution. The latter can be easily obtained by applying Faraday's law to the measured evolved hydrogen. Furthermore, with this methodology, it is possible to measure the amount of hydrogen evolved during polarisation, and also to examine the hydrogen evolution transient after the external current is interrupted, in order to evaluate directly the phenomenon of cathodic activation.

RESULTS

Figure 2 presents the behaviour recorded for high purity aluminium (99.99 wt.%) and AA2024-T3 during potentiodynamic polarisations and hydrogen evolution measurements. Since in aerated conditions corrosion proceeds at the pitting potential for both materials, upon anodic polarisation the current rapidly increased to values above 0.1 mA cm^{-2} due to the immediate onset of stable pitting. At higher polarisations, the rate of increase of current with applied potential decreased, indicating the onset of Ohmic control. The behaviour of the current associated with hydrogen evolution was closely similar to the electrical response, with a faster increase for small polarisations, followed by a region of less marked increase of current with applied potential. When the anodic polarisation was interrupted (Fig. 3a), at 1 V vs. SCE, a very sharp decrease in the current associated with hydrogen evolution was observed, with a drop from 0.2–0.3 mA cm^{-2} to approximately one order of magnitude less. A similar overall behaviour was observed for the AA2024-T3 alloy, with the only major difference observed at the end of the polarisation experiment (Figs. 2 and 3a). It is worth to mention that for the practical alloy, when the anodic polarisation was interrupted, a progressive decrease in the current associated with hydrogen evolution was observed, rather than the sharp drop typical of pure aluminium. In both cases, however, during anodic polarisation, the current associated with hydrogen evolution was lower than the current measured by the electrical circuit.

When performing cathodic polarisation on the two materials, a markedly different behaviour was observed (Fig. 1). For pure aluminium, during cathodic polarisation, the current measured by the potentiostat was initially relatively low, due to the absence (or very limited presence) of cathodically active intermetallics supporting oxygen reduction. The current increased progressively from values of the order of to 10^{-5} mA cm^{-2}, close to the corrosion potential, to values in the region of 10^{-2} mA cm^{-2} for potentials close to −1.6 V vs. SCE, where macroscopic cathodic hydrogen evolution become evident. With the onset of cathodic hydrogen evolution, a sharp increase in the current measured by the potentiostat was observed, together with a sharp increase in the current associated with hydrogen evolution. Interestingly, at potential more negative than −1.6 V vs. SCE, once abundant hydrogen evolution was initiated, the current associated with hydrogen evolution was larger than the current measured by the potentiostat. This indicates that together with Faradic hydrogen evolution at potentials more negative than −1.6 V vs. SCE, additional processes occurred on the metal surface, and an excess of hydrogen gas was produced with respect to the applied cathodic current. Similarly to the case of anodic polarisation, when the cathodic polarisation of aluminium was terminated, a sharp decrease in current associated with hydrogen evolution was observed (Fig. 3b), with the value of current approaching immediately the background noise of the hydrogen detection system.

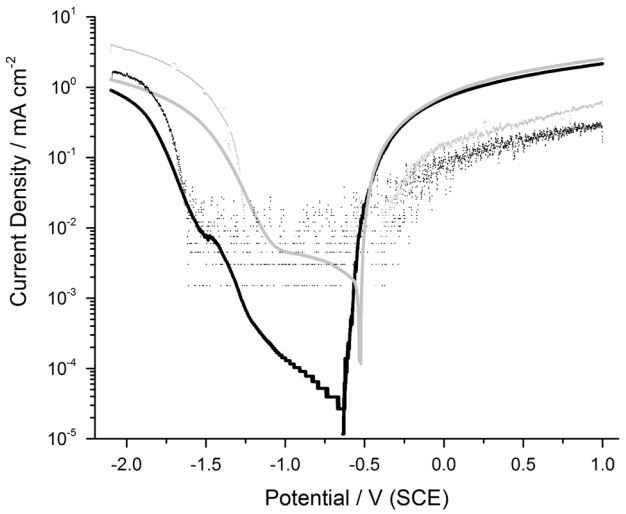

Fig. 2 Potentiodynamic response of aluminium (*black*) and AA2024-T3 (*light-grey*). Solid lines represent the current response measured by the potentiostat, points represent the current associated with hydrogen evolution measured by the gravimetric method

Cathodic polarisation of the AA2024-T3 alloy (Fig. 2) revealed a significantly different behaviour. In particular, the electrical response showed a region of diffusion-limited oxygen reduction that extended up to approximately −1.1 V vs. SCE, where abundant cathodic hydrogen evolution was onset. The fact that the hydrogen measurement setup recorded a current that is similar to the diffusion limited oxygen current is a coincidence, consequence of the resolution limitation of the hydrogen measurement device, and it is not a relevant finding deserving further discussion. However, after the macroscopic cathodic hydrogen evolution was initiated below −1.1 V vs. SCE, similarly to the case of pure aluminium, a sharp increase in both the electrical current and in the current associated with the hydrogen evolution was observed. The sharp increase in current density occurs at potential less cathodic for the alloy compared to pure aluminium, because the copper-rich, cathodically active, intermetallics present on the alloy surface require lower overpotential than pure aluminium to support abundant hydrogen evolution. As for pure aluminium, also for the alloy, the current associated with hydrogen was larger than the cathodic current supplied by the potentiostat, after macroscopic cathodic hydrogen evolution was onset. Upon termination of the cathodic polarisation of the alloy (Fig. 3b), a behaviour different from that observed in all the previous cases was revealed; specifically, both a first sharp drop in the current associated with hydrogen evolution was revealed, followed by a long transient, when the hydrogen current progressively decreased.

Summarising the findings, during anodic polarisation, superfluous hydrogen evolution was observed on pure aluminium and on the alloy, with the main difference between the two materials being the increased amount of hydrogen evolved from the alloy and the long transient in the hydrogen current observed for the alloy after the termination of the polarisation. During cathodic polarisation, superfluous hydrogen evolution was also observed on both materials, with the main difference being the potential associated with the onset of hydrogen evolution (less cathodic for AA2024-T3), the increased amount of hydrogen for the alloy, and the longer transient in hydrogen current observed after the interruption of the polarisation of the alloy. For both materials, the absolute value of the current associated with hydrogen evolution was lower than the electrical current during anodic polarisation and higher during cathodic polarisation. In fact, during cathodic polarisation, in an ideal case (or on Pt for instance), the electrical and hydrogen current should coincide. Here, for the first time, it was observed that also during cathodic polarisation of aluminium superfluous hydrogen can be generated.

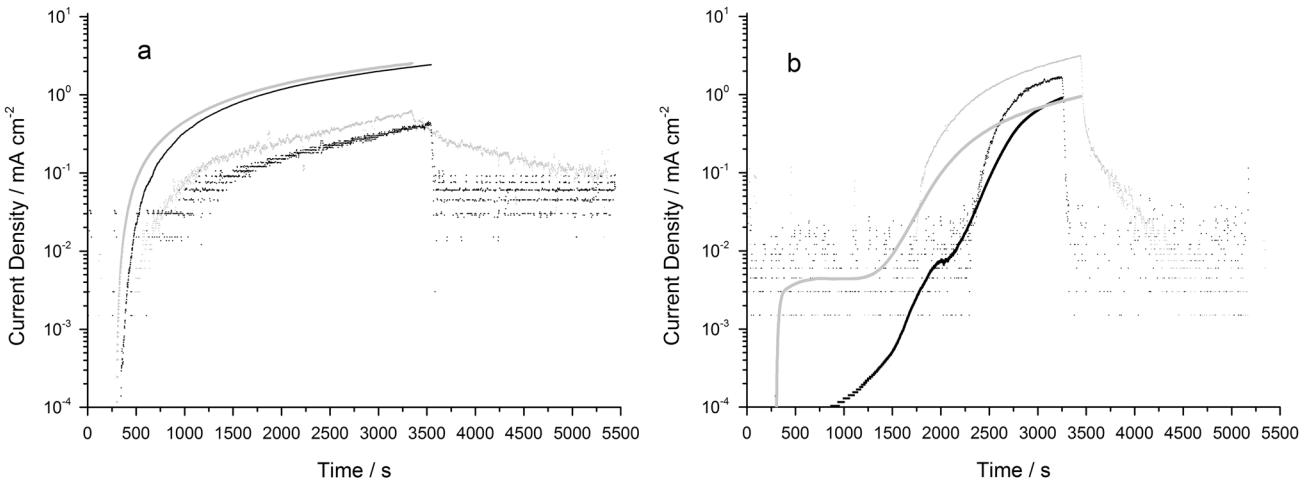

Fig. 3 Time evolution of the absolute value of current associated with hydrogen evolution for aluminium (*black*) and AA2024-T3 (*light-grey*). *Solid lines* represent the current response measured by the potentiostat during polarisation, *points* represent the current associated with hydrogen evolution measured by the gravimetric method before, during and after polarisation; **a** anodic polarisation and **b** cathodic polarisation

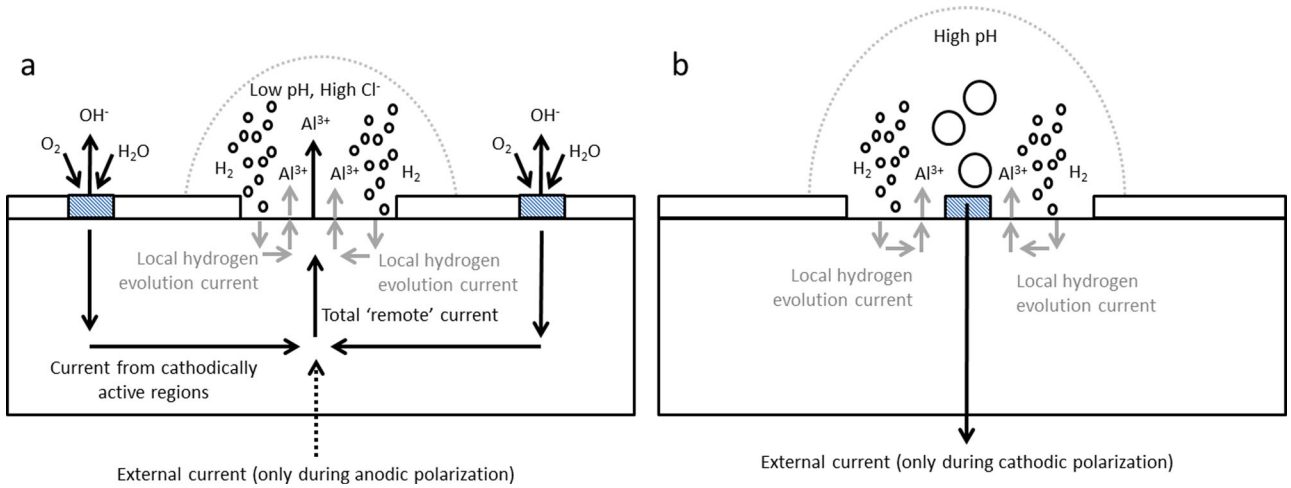

Fig. 4 Schematic representation of the processes inducing superfluous hydrogen evolution during **a** anodic polarisation and **b** cathodic polarisation

DISCUSSION

When an anodic current is applied to an aluminium electrode in the presence of depassivating conditions (for example chlorides), the oxide film that naturally forms and protects the metal is locally damaged. At the locations where the film is damaged, the solution can come in contact with the metal and hydrogen evolution can take place due to the large potential difference available between aluminium oxidation and hydrogen evolution. It should be noted that the macroscopic electrode potential does not reflect the value of the potential at the locations where the film is ruptured, since a large ohmic drop is introduced locally by the relatively large current exiting the metal from a relatively small area. The overall effect at the active site is a current amplifier, schematically depicted in Fig. 4a, where the total current associated with metal oxidation is the sum of the current that arrives to the corrosion front from a remote location (external circuit or cathodically active regions far from the corrosion front), and the cathodic current generated locally by hydrogen evolution on the depassivated regions. As a result, when the electrical anodic current is increased such as during anodic potentiodynamic polarisation, the depassivated area becomes larger, and an increase in current associated with hydrogen evolution is observed ('anodic' superfluous hydrogen evolution). The described model accounting for '*anodic*' superfluous hydrogen evolution was introduced previously and applies well to both aluminium and magnesium under a variety of experimental conditions.[12, 22, 23, 28]

In this work, for the first time, a similar process resulting in superfluous hydrogen evolution has been also observed during cathodic polarisation ('*cathodic*' superfluous hydrogen evolution). During cathodic polarisation, initially, oxygen reduction occurs on the electrode surface, with a kinetic dependent on the surface properties and composition. When the cathodic potential required for macroscopic hydrogen evolution is attained (circa −1.6 V vs. SCE for aluminium and −1.1 V vs. SCE for AA2024-T3), the process initiates and strong local alkalinisation nearby the cathodically active regions occurs. Recalling the Pourbaix diagram of aluminium, such alkalinisation can lead to the attack of the air-formed oxide and, similarly to the case of anodic polarisation, to the exposure of the metal to the electrolyte, as schematically illustrated in Fig. 4b.

Once this happens, due to the large difference available between the electrochemical potential of aluminium oxidation and that of hydrogen evolution, the two phenomena both progress at the activated sites. As a consequence, during cathodic

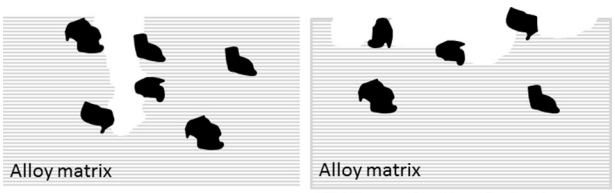

Fig. 5 Schematic representation of the phenomena leading to cathodic activation **a** after anodic polarisation and **b** after cathodic polarisation. Dark particles represent the cathodically-active, copper-rich second phases

polarisation, an excess of hydrogen compared to the current applied is observed, together with some oxidation of aluminium. It is evident that, comparing Figs. 4a and 4b, the model based on surface film damage proposed for the '*anodic*' superfluous hydrogen evolution can be applied also to the '*cathodic*' superfluous hydrogen evolution, with the difference that the direction of the '*remote*' current is inverted. The direct effect of the cathodic '*remote*' current is to sustain directly hydrogen evolution, which produces local alkalinisation. As a result of the alkalinisation the oxide film becomes unstable and additional local hydrogen evolution and aluminium oxidation are induced.

The effects of the presence of cathodically active elements within the practical alloy can be considered by comparing the anodic and cathodic responses of the AA2024-T3 alloy with the responses of the high purity aluminium. During anodic polarisation, the presence of the more noble alloying elements in the alloy only had a minor effect on the ratio between the applied anodic current and the amount of current produced by hydrogen evolution. In particular, for large values of polarisation, the ratio between electrical current and hydrogen current was about 8 for high purity aluminium and about 5 for the AA2024-T3. A similar observation could be made during cathodic polarisation, where for large values of polarisation the ratio between the electrical current and the hydrogen current was 0.4–0.5 for high purity aluminium, and in the region of 0.32–0.35 for the alloy. Thus, both during anodic and cathodic polarisation, the presence of more noble alloying elements compared to aluminium resulted in a slightly increased tendency to hydrogen evolution, which is compatible with the idea that once the oxide film is removed from the surface, by either an anodic or cathodic process, the presence of alloying elements with low overpotential for hydrogen evolution within the aluminium matrix results in a slight increase in the amount of superfluous hydrogen evolution. Additionally, it should be noted that where hydrogen evolution takes place, the local potential is always well below that associated with copper oxidation. Thus, at the active corrosion front, metallic copper enrichment can occur both by preferential oxidation of aluminium and by local redeposition of copper ions present in the environment.

By observing the transients in the current associated with hydrogen evolution after the polarisation is interrupted, the effect of alloying elements on cathodic activation can be rationalised. For both anodic and cathodic polarisation of high purity aluminium, after the external current is interrupted a sharp drop of the current associated with hydrogen evolution close to the detection limit values is observed. This result suggest that, regardless of the mechanism inducing the superfluous hydrogen evolution and the oxidation of aluminium (anodic or cathodic polarisation), the increase in cathodic activity of the aluminium surface is negligible, or at least below the detection limit of the instrumentation used in this work. This can be rationalised by considering that pure aluminium contains only a very low amount of iron-rich intermetallics exposed to the electrolyte and, even if preferential oxidation of aluminium matrix occurs, the increase in surface population of such intermetallics is not substantial.

Vice versa, significant cathodic activation is observed for the copper-containing alloy. After termination of the anodic polarisation, it is evident from the fact that the current associated with hydrogen evolution remains relatively high and exhibits a long transient. This can be rationalised considering that the oxidation occurring during anodic polarisation results in the accumulation of cathodically active material on the alloy surface, such as exposed second phase particles and copper-rich layer, together with the formation of stable pits within the alloy as schematically depicted in Fig. 5a. When the external polarisation is interrupted, stable pits that are locally acidified are present on the surface, together with cathodically active regions generated by selective oxidation of aluminium. Thus, the cathodically active regions generate a relatively large cathodic current (either by oxygen reduction or hydrogen evolution), that maintains active the corrosion front, where additional hydrogen is evolved. As time progresses, the active corrosion sites generated during anodic polarisation have to compete for the available '*remote*' current produced on the electrode surface. Once the remote current becomes limited, at some sites, the alkalinisation from the hydrogen evolution will dominate over the acidification due to the anodic reaction, and passivity can be re-established. Thus some of the active sites stop propagating, and a progressive reduction in current associated with hydrogen evolution is observed.

More complex is the hydrogen evolution behaviour observed after the termination of the cathodic polarisation. Here, the attack of the aluminium matrix due to alkalinisation has occurred next to the intermetallics (Fig. 5b), resulting in significant increase in their surface population. As soon as the cathodic polarisation is terminated, the current associated with hydrogen evolution exhibits a sharp decrease. This can be rationalised considering that the total value of hydrogen current measured is given by the sum of i) the hydrogen current induced directly by the external cathodic current, plus ii) the hydrogen resulting from the local processes that are consequence of alkalinisation. When the external polarisation is interrupted, the sharp decrease in the measured hydrogen current is due to the fact that the first contribution is instantaneously removed. Thus, after the termination of the polarisation, the residual hydrogen evolution is due to the hydrogen evolving from the alkaline depassivated regions (where aluminium oxidises), and from the (alkaline) cathodically active regions, such as those with increased amount of exposed second phase material, generated previously by selective oxidation of the aluminium matrix. With time, some of the active anodic sites will stabilise, sustained by the cathodic processes occurring on the large amount of newly exposed intermetallics, initiating a process similar to that described above after termination of anodic polarisation. Overall, cathodic activation is not observed for pure aluminium but it is observed for the copper-containing alloy, both after anodic and cathodic polarisation. This indicates that hydrogen evolution is more persistent in the presence of more noble elements, regardless of the mechanism that has induced film rupture and the preferential oxidation of the aluminium matrix.

In summary, this work investigated the hydrogen evolution behaviour of high purity aluminium and AA2024-T3 alloy during anodic and cathodic polarisation. For the first time, superfluous hydrogen evolution occurring during anodic polarisation was quantified directly and, also for the first time, it was disclosed that superfluous hydrogen evolution occurs also during cathodic polarisation. Superfluous hydrogen evolution from both '*anodic*' and '*cathodic*' polarisation can be rationalised considering that, for different reasons (i.e. pH alteration or dynamic changes in local chloride concentration), the air formed film separating the metal from the electrolyte is locally altered, damaged or absent. At such locations, due to the large difference in potential between

aluminium oxidation and hydrogen evolution, local hydrogen evolution takes place, generating '*superfluous*' hydrogen. Thus, the damage or removal of surface film, regardless of the mechanism that has induced it, can result in the generation of superfluous hydrogen evolution. The presence of cathodically active alloying elements within the alloy also facilitates hydrogen evolution during both anodic and cathodic polarisation, and produces the phenomenon of cathodic activation. The cathodic activation on the AA2024-T3 alloy is evident as a significant rate of residual hydrogen evolution after the polarisation (anodic or cathodic) has been terminated, and was not observed for pure aluminium.

METHODS

Materials and reagents

Aluminium 99.99 wt.% and AA2024-T3 (nominal composition Cu 4.5-wt.%, Mg 1.44 wt.%, Mn 0.60 wt.%, Si 0.06 wt.%, Fe 0.13 wt.%, Zn 0.02 wt.%, Ti 0.03 wt.%, Al balance) specimens were cut from 0.9 and 1.6 mm sheets respectively. After cutting, they were degreased in acetone for 10 min and stored in a desiccator until needed. Before testing, each specimen was electrically connected to an insulated copper wire and masked with beeswax, such as an area of 12 cm^2 was exposed to the test electrolyte. The test electrolyte was prepared by adding 35 g l^{-1} of NaCl to deionised water. Fresh solutions and new specimens were employed for each test.

Gravimetric method

In order to acquire real-time measurement of the hydrogen evolved during potentiodynamic polarisation the gravimetric method was used. The method, schematically depicted in Fig. 1, is described in detail elsewhere [21–23, 25] and only outlined briefly here. The electrode under study is attached to a rigid rod, below a hydrogen collecting cylinder rigidly connected to the same rod. The assembled electrode, rod and hydrogen collecting cylinder form a single component that is immersed in the test solution, such as the top of the hydrogen collecting cylinder is below the solution surface. The non-immersed side of the rod is then attached to a suspended laboratory balance, to record its weight, and the cable is connected to the working electrode terminal of the potentiostat. Immediately after immersion, the air present inside the hydrogen collecting cylinder is removed by using a syringe and a curved plastic tube, such as the cylinder is filled completely with the test solution. With this setup, the hydrogen evolved from the electrode surface accumulates in the collecting cylinder and a buoyancy force, acting on the rod connected to the balance, is generated. Such buoyancy force modifies the weight that is recorded by the balance. Consequently, by recording the weight as a function of time it is possible to calculate a value of current associated with hydrogen evolution by using Faraday's law.

Electrochemical measurements

Electrochemical measurements were performed by using a classical 3 electrode cell, with the aluminium or alloy specimen as working electrode, a saturated calomel electrode as reference and a platinum counter electrode. All measurements were performed at room temperature and in stagnant solutions by using an Iviumstat potentiostat and repeated a minimum of three times. The reproducibility between measurements conducted under nominally identical conditions was excellent, with curves almost overlapping. The potentiodynamic polarisation measurements were recorded after 1800 s of free corrosion in the test solution. The hydrogen measurement was initiated 300 s before the potentiodynamic polarisation started. The balance used was a Mettler Toledo MS204TS. Finally, all potentiodynamic polarisations were initiated at the free corrosion potential and terminated at 1 V vs. SCE (anodic) and −2 V vs. SCE (cathodic), and were performed at a scan rate of 0.5 mV s^{-1}.

ACKNOWLEDGEMENTS

We thank EPSRC and the STEPFAR for financial support. The present work has been funded by EPSRC, LATEST2 Programme Grant (EP/H020047/1) and of the STEPFAR Programme Grant (PON 03PE_00129_1)

AUTHOR CONTRIBUTIONS

C.L. optimised the experimental setup and performed the electrochemical testing, M.C. and F.S. contributed to experimental design, data analysis and manuscript preparation, F.B. and T.M. contributed to data analysis and manuscript preparation.

ADDITIONAL INFORMATION

Competing interests: The authors declares that they have no competing financial interests.

Publisher's note: Springer Nature remains neutral with regard to jurisdictional claims in published maps and institutional affiliations.

REFERENCES

1. Pourbaix, M. Applications of electrochemistry in corrosion science and in practice. *Corros. Sci.* **14**, 25–82 (1974).
2. Lebouil, S. *et al*. A novel approach to on-line measurement of gas evolution kinetics: application to the negative difference effect of Mg in chloride solution. *Electrochim. Acta* **124**, 176–182 (2014).
3. Frankel, G. S., Samaniego, A. & Birbilis, N. Evolution of hydrogen at dissolving magnesium surfaces. *Corros. Sci.* **70**, 104–111 (2013).
4. Williams, G., Birbilis, N. & McMurray, H. N. The source of hydrogen evolved from a magnesium anode. *Electrochem. Commun.* **36**, 1–5 (2013).
5. Kirkland, N. T., Williams, G. & Birbilis, N. Observations of the galvanostatic dissolution of pure magnesium. *Corros. Sci.* **65**, 5–9 (2012).
6. King, A. D., Birbilis, N. & Scully, J. R. Accurate electrochemical measurement of magnesium corrosion rates; A combined impedance, mass-loss and hydrogen collection study. *Electrochim. Acta* **121**, 394–406 (2014).
7. Song, G. & StJohn, D. The effect of zirconium grain refinement on the corrosion behaviour of magnesium-rare earth alloy MEZ. *J. Light Met.* **2**, 1–16 (2002).
8. Cao, F. *et al*. Corrosion of ultra-high-purity Mg in 3.5% NaCl solution saturated with Mg(OH)2. *Corros. Sci.* **75**, 78–99 (2013).
9. Qiao, Z., Shi, Z., Hort, N., Zainal Abidin, N. I. & Atrens, A. Corrosion behaviour of a nominally high purity Mg ingot produced by permanent mould direct chill casting. *Corros. Sci.* **61**, 185–207 (2012).
10. Glenn, A. M. *et al*. Corrosion of AA2024-T3 Part III: propagation. *Corros. Sci*. 53, 40–50.
11. Hughes, A. E. *et al*. Corrosion of AA2024-T3 Part II: co-operative corrosion. *Corros. Sci.* 53, 27–39
12. Curioni, M. & Scenini, F. The mechanism of hydrogen evolution during anodic polarization of aluminium. *Electrochim. Acta* **180**, 712–721 (2015).
13. Frankel, G. S., Fajardo, S. & Lynch, B. M. Introductory lecture on corrosion chemistry: a focus on anodic hydrogen evolution on Al and Mg. *Faraday Discuss.* **180**, 11–33 (2015).
14. Bargeron, C. B. & Benson, R. C. Analysis of the gases evolved during the pitting corrosion of aluminum in various electrolytes. *J. Electrochem. Soc.* **127**, 2528–2530 (1980).
15. de Wexler, S. B. & Galvele, J. R. Anodic behaviour of aluminium straining and mechenism for pitting. *J. Electrochem. Soc.* **121**, 1271–1276 (1974).
16. Dražić, D. M. & Popić, J. Hydrogen evolution on aluminium in chloride solutions. *J. Electroanal. Chem.* **357**, 105–116 (1993).
17. Frankel, G. S. The growth of 2-D pits in thin film aluminum. *Corros. Sci.* **30**, 1203–1218 (1990).
18. Dražić, D. M. & Popić, J. P. Corrosion rates and negative difference effects for Al and some Al alloys. *J. Appl. Electrochem* **29**, 43–50 (1999).
19. Despić, A. R., Dražić, D. M., Purenović, M. M. & Ciković, N. Electrochemical properties of aluminium alloys containing indium, gallium and thallium. *J. Appl. Electrochem.* **6**, 527–542 (1976).
20. Scala, A. *et al*. Corrosion fatigue on 2024T3 and 6056T4 aluminum alloys. *Surf. Interface Anal.* **42**, 194–198 (2010).
21. Curioni, M. The behaviour of magnesium during free corrosion and potentiodynamic polarization investigated by real-time hydrogen measurement and optical imaging. *Electrochim. Acta* **120**, 284–292 (2014).
22. Curioni, M., Scenini, F., Monetta, T. & Bellucci, F. Correlation between electrochemical impedance measurements and corrosion rate of magnesium investigated by real-time hydrogen measurement and optical imaging. *Electrochim. Acta* **166**, 372–384 (2015).
23. Curioni, M., Torrescano-Alvarez, J., Yang, Y. & Scenini, F. Application of side-view imaging and real-time hydrogen measurement to the investigation of magnesium corrosion. *Corrosion* **73**, 463–470 (2016).
24. Fajardo, S. & Frankel, G. S. Effect of impurities on the enhanced catalytic activity for hydrogen evolution in high purity magnesium. *Electrochim. Acta* **165**, 255–267 (2015).

25. Fajardo, S. & Frankel, G. S. Gravimetric method for hydrogen evolution measurements on dissolving magnesium. *J. Electrochem. Soc.* **162**, C693–C701 (2015).
26. Fajardo, S., Glover, C. F., Williams, G. & Frankel, G. S. The source of anodic hydrogen evolution on ultra high purity magnesium. *Electrochim. Acta* **212**, 510–521 (2016).
27. Rossrucker, L. *et al*. The pH dependence of magnesium dissolution and hydrogen evolution during anodic polarization. *J. Electrochem. Soc.* **162**, C333–C339 (2015).
28. Yang, Y., Scenini, F. & Curioni, M. A study on magnesium corrosion by real-time imaging and electrochemical methods: Relationship between local processes and hydrogen evolution. *Electrochim. Acta* **198**, 174–184 (2016).
29. Song, G., Atrens, A., St. John, D., Wu, X. & Nairn, J. The anodic dissolution of magnesium in chloride and sulphate solutions. *Corros. Sci.* **39**, 1981–2004 (1997).
30. Song, G., Atrens, A., Stjohn, D., Nairn, J. & Li, Y. The electrochemical corrosion of pure magnesium in 1 N NaCl. *Corros. Sci.* **39**, 855–875 (1997).
31. McCafferty, E. Sequence of steps in the pitting of aluminum by chloride ions. *Corros. Sci.* **45**, 1421–1438 (2003).
32. Frankel, G. S., Fajardo, S. & Lynch, B. M. Introductory lecture on corrosion chemistry: a focus on anodic hydrogen evolution on Al and Mg. *Faraday Discuss.* **180**, 11–33 (2015).
33. Liu, R., Thomas, S., Scully, J., Williams, G. & Birbilis, N. An experimental survey of the cathodic activation of metals including Mg, Sc, Gd, La, Al, Sn, Pb and Ge in dilute chloride solutions of varying pH. *Corrosion* **73**, 494–505 (2017).
34. Williams, G. & Neil McMurray, H. Localized corrosion of magnesium in chloride-containing electrolyte studied by a scanning vibrating electrode technique. *J. Electrochem. Soc.* **155**, C340–C349 (2008).